Morphologic Features of Crystalline Lens in Patients with Primary Angle Closure Disease Observed by CASIA 2 Optical Coherence Tomography

Xiaolei Wang,[1,2] Xiaoxiao Chen,[1,2] Yizhen Tang,[1,2] Jiajian Wang,[1] Yuhong Chen,[1–3] and Xinghuai Sun[1–4]

[1]Department of Ophthalmology and Visual Science, Eye, Ear, Nose and Throat Hospital, Shanghai Medical College of Fudan University, Shanghai, China
[2]NHC Key Laboratory of Myopia, Ministry of Health (Fudan University), Shanghai, China
[3]Shanghai Key Laboratory of Visual Impairment and Restoration (Fudan University), Shanghai, China
[4]State Key Laboratory of Medical Neurobiology, Institutes of Brain Science, and Collaborative Innovation Center for Brain Science, Fudan University, Shanghai, China

Correspondence: Yuhong Chen, Department of Ophthalmology and Visual Science, Eye, Ear, Nose and Throat Hospital, Shanghai Medical College of Fudan University, Shanghai 200031, China; yuhongchen@fudan.edu.cn.
Xinghuai Sun, Department of Ophthalmology and Visual Science, Eye, Ear, Nose and Throat Hospital, Shanghai Medical College of Fudan University, Shanghai 200031, China; xhsun@shmu.edu.cn.

XW and XC contributed equally to this work and are regarded as first authors.
YC and XS contributed equally to the work presented here and are regarded as corresponding authors.

Received: November 3, 2019
Accepted: April 2, 2020
Published: May 22, 2020

Citation: Wang X, Chen X, Tang Y, Wang J, Chen Y, Sun X. Morphologic features of crystalline lens in patients with primary angle closure disease observed by CASIA 2 optical coherence tomography. *Invest Ophthalmol Vis Sci.* 2020;61(5):40. https://doi.org/10.1167/iovs.61.5.40

Purpose. To investigate the morphologic features of crystalline lens in primary angle closure disease (PACD) by the swept-source anterior segment optical coherence tomography.

Methods. This cross-sectional observational study included 125 consecutive eyes from 125 patients who underwent anterior segment optical coherence tomography (CASIA 2, Tomey, Nagoya, Japan) examination, including 38 eyes of normal controls, 57 eyes of PAC suspects (PACS), and 30 eyes with PAC or PAC glaucoma (PACG). Crystalline lens parameters were compared among the three groups. Spearman correlation analysis and multiple linear regression models were performed to evaluate the relationships between the lens parameters and related factors.

Results. Significant differences were found for anterior chamber depth, axial length, iridotrabecular contact index, lens vault, lens thickness (all $P < 0.001$), the anterior radius curvature of lens (normal vs PACS vs PAC/PACG: 9.35 ± 1.29 mm vs 8.40 ± 0.62 mm vs 8.12 ± 0.54 mm; $P < 0.001$), lens decentration (normal vs PACS vs PAC/PACG: 0.14 ± 0.07 mm vs 0.19 ± 0.09 mm vs 0.22 ± 0.12 mm; $P = 0.004$), and tilt (normal vs PACS vs PAC/PACG: 4.9 ± 1.0° vs 5.3 ± 1.2° vs 5.8 ± 1.8°; $P = 0.033$) among the three groups. The multivariate regression analysis found that both iridotrabecular contact index and the stage of the PACD were negatively correlated with the anterior radius curvature of lens, positively correlated with lens thickness and decentration after adjustment for age, sex, and axial length (all $P < 0.05$).

Conclusions. Steep anterior curvature and decentration of the crystalline lens may be another anatomic characteristic of eyes with PACD. These findings support that the crystalline lens morphologic features may have great contribution to the development of PACD.

Keywords: primary angle closure disease, anterior segment optical coherence tomography, crystalline lens, CASIA 2

Glaucoma is the second leading cause of vision loss in the world with an estimated 67 million people affected. Nearly one-half of these cases are primary angle closure glaucoma (PACG),[1] which has the highest prevalence in Asian.[2,3] Although PACG can cause severe visual impairment if untreated, it can be cured or well controlled when in early stage such as primary angle closure suspect (PACS), as well as primary angle closure (PAC). PACG, PAC and PACS can be classified into primary angle closure disease (PACD).[4]

Biometric studies have shown that PACD has a shallow anterior chamber depth (ACD) and a short axial length (AL).[5–7] Pupillary block and nonpupillary block have been proposed as two main mechanisms underlying the pathogenesis of PACD.[8–10] Furthermore, previous studies have also demonstrated that the crystalline lens plays an important role in the development of PACG, such as the lens thickness (LT) and relative lens position.[5,11–16] However, the distribution and change of lens morphologic features during the progression of PACD remains unclear.

In recent years, a new generation of swept-source anterior segment optical coherence tomography (AS-OCT, CASIA 2, Tomev Corporation, Nagoya, Japan) has come into use. It has a wide scanning range of 16 mm, which allows an entire cross-section of the anterior and posterior lens surface to be

captured simultaneously. It can calculate the detailed parameters of lens, including the anterior and posterior curvatures, the decentration and the tilt of the lens. In the current study we aimed to explore the lens morphologic features in different stages of PACD by using the CASIA 2.

Methods

Participants

All participants in the study were enrolled from the glaucoma clinic of Eye, Ear, Nose and Throat Hospital of Fudan University (Shanghai, China). This cross-sectional, comparative study was approved by the Ethical Review Committee of the Eye, Ear, Nose and Throat Hospital and it adhered to the Declaration of Helsinki for Research Involving Human Participants. Written informed consent was obtained from each participant involved in the study. All participants were from the Chinese Han population.

Participants diagnosed as PACS, PAC, and PACG were included.[4,17] PACS was defined as an eye with pigmented trabecular meshwork invisible for 180° or greater under static gonioscopy but without peripheral anterior synechiae, IOP, or glaucomatous optic neuropathy. Peripheral anterior synechiae was defined as a region of iridotrabecular contact that could not be opened by indentation gonioscopy.[18] PAC was defined as an eye with presence of peripheral anterior synechiae or elevated IOP, but without glaucomatous optic neuropathy. PACG was defined as an eye with PAC and glaucomatous optic neuropathy. When both eyes of one patient met the criteria, the eye in the more advanced stage or with better image quality was included for analysis.

The inclusion criteria for the normal subjects were as follows: open angle, normal-appearing optic nerve head; intact neuroretinal rim and retinal nerve fiber layer; normal standard automated perimetry; and no records of elevated IOP of more than 21 mm Hg.

Patients who (1) had incisional surgery or laser peripheral iridotomy (LPI) in either eye (including cataract surgery), (2) had histories of eye diseases (such as uveitis, trauma), or (3) under the use of pilocarpine were excluded.

Ophthalmic Examination and AS-OCT Imaging

Participants underwent a complete ophthalmic examination, including a review of their medical history, measurements of best-corrected visual acuity (BCVA), refractive status, slit-lamp biomicroscopy, IOP (Goldmann applanation tonometry), fundoscopy (TRC-NW200, Topcon Medical Systems, Oakland, NJ), ultrasound biomicroscopy, gonioscopy, central corneal thickness (CCT) and AL (Lenstar, Carl Zeiss Inc., Jena, Germany), retinal nerve fiber layer, ganglion cell complex thickness (RTvue OCT; Optovue Inc, Toledo, OH), and visual field (Humphrey Field Analyzer, 24-2; Carl Zeiss Meditec, Dublin, CA). The mean spherical equivalence (MSE) was calculated as the spherical diopter plus one-half of the cylindrical dioptric power. The lens opacity of each eye was graded using the Lens Opacities Classification System III standards. The nuclear opalescence (NO), nuclear color (NC), cortical (C), and posterior subcapsular (P) cataract were compared with the standard grading color photographs. NO and NC were graded on a scale of 1 to 6, C and P were graded on a scale of 1 to 5.[19]

All subjects underwent AS-OCT (CASIA 2, Tomey Corporation, Nagoya, Japan) imaging before any contact procedure. The CASIA 2 uses a 1310 nm wavelength swept-source laser at a frequency of 0.3 seconds, producing 16 AS-OCT images from 16 different angles. Each two-dimensional image exhibits the anterior and posterior curvature of lens (*yellow lines*), which are extended to intersect at two symmetrical points and thus the outline of the lens is obtained (Fig. 1). The 16 different two-dimensional angle images are then analyzed to obtain the three-dimensional crystalline lens morphology and lens parameters: front Rs (the anterior radius of steep curvature of the lens), front Rf (the anterior radius of flat curvature of the lens), front R (mean value of anterior Rs and Rf of the lens), back Rs (the posterior radius of steep curvature of the lens), back Rf (the posterior radius of flat curvature of the lens), back R (mean value of posterior Rs and Rf of the lens), thickness (LT along vertex normal), diameter (diameter of equator part of the lens), and lens vault (LV, vertical distance from the anterior lens surface to the horizontal line connecting the two scleral spurs). The methods of decentration and tilt of lens had been reported previously.[20] The decentration was the vertical distance from lens center to vertex normal, and the tilt was the angle of lens axis against vertex normal (Fig. 2). The vertex normal was the line between the fixation point and the vertex of corneal topographic map. The decentration data were presented as γ (mm), Δ (degree), where γ represents the lens decentration from the corneal topographic axis, and Δ represents its azimuth. The tilt data are

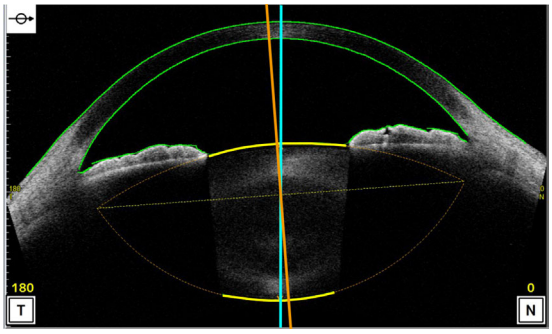

Figure 1. The image of anterior segment captured by CASIA 2. The two-dimensional image exhibits the anterior and posterior curvature of lens (*yellow lines*), which are extended to intersect at two symmetrical points and thus the outline of the lens is obtained (lens axis, *orange line*; vertex normal, *blue line*).

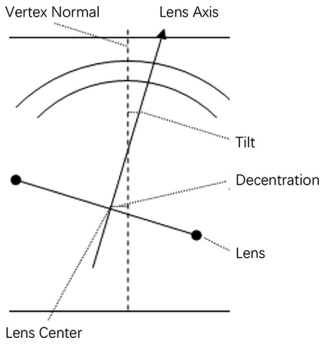

Figure 2. The diagram showing the method of decentration and tilt of the lens. Decentration was the vertical distance from lens center to vertex normal. Tilt was the angle of lens axis against vertex normal. The vertex normal was the line between the fixation point and the vertex of corneal topographic map.

Table 1. Clinical Characteristics of the Study Participants

Characteristic	Normal ($n = 38$)	PACS ($n = 57$)	PAC/PACG ($n = 30$)	P Value*
Sex (male:female)	13:25	12:45	5:25	0.189
Age, years	58.3 ± 7.2	61.4 ± 6.2	62.0 ± 10.1	0.077
BCVA, LogMAR	0.16 ± 0.22	0.17 ± 0.28	0.48 ± 0.51	<0.001
MSE, diopters	0.004 ± 0.5	0.3 ±0.6	0.5 ±0.7	0.006
IOP, mmHg	16.2 ± 3.3	15.9 ± 3.9	21.7 ± 10.1	<0.001
ACD, mm	2.54 ± 0.34	2.08 ± 0.22	1.93 ± 0.24	<0.001
CCT, µm	540.6 ± 35.1	533.2 ± 33.7	539.7 ± 45.5	0.577
NO	1.1 ± 1.0	1.4 ± 1.0	1.9 ± 1.3	0.006
NC	1.1 ± 1.0	1.4 ± 0.9	2.0 ± 1.4	0.003
C	1.6 ± 0.9	2.0 ±0.9	2.3 ±1.2	0.010
P	1.6 ± 0.8	1.9 ± 0.7	2.2 ± 1.1	0.007
AL, mm	23.14 ± 0.87	22.47 ± 0.86	22.34 ± 0.73	<0.001
ITC Index, %	11.4 ± 14.7	41.1 ± 26.2	63.0 ± 24.5	<0.001

Values are mean ± standard deviation.
* All calculated by one-way ANOVA, except the sex was calculated by the χ^2 test.

presented as α (degree), β (degree), where α represents the lens tilt from the corneal topographic axis, and β represents its azimuth. The irido-trabecular contact (ITC) index was the rate of contact between the iris and angle wall anterior to the scleral spur over 360°. The best quality image among three captures was chosen for analysis. All images were processed using inbuilt semiautomated software by a single experienced observer who was masked to clinical data. The scleral spurs were determined by two glaucoma specialists (XW and YC).

Statistical Analysis

All analyses were performed using an open source R statistical software (version 3.4.3; The R Foundation, Vienna, Austria). Numerical variables were shown as mean ± standard deviation. The ANOVA test and the Kruskal-Wallis test were used to compare the differences among the three groups according to the data distribution. The Spearman correlation analysis and multiple linear regression models were performed to evaluate the relationships between the lens parameters and related factors. Tests for trend were performed by entering the categorical variables as continuous parameters in the models. Restricted cubic spline was used to estimate the dose–response relation of ITC index and lens parameters. The significance level was set at $P < 0.05$.

Results

A total of 135 eyes of 135 subjects were enrolled in the study. Ten subjects had to be excluded because of poor image quality for both eyes, so 125 eyes were analyzed: 38 eyes were normal controls, 57 eyes were PACS, and 30 eyes were PAC/PACG (Supplementary Table S1). The demographic and basic clinic information of the three groups were shown in Table 1. There were no significant differences in sex, age, and CCT among three groups (all $P > 0.05$). However, statistically significant differences were found for BCVA ($P < 0.001$), MSE ($P = 0.006$), IOP ($P < 0.001$), ACD ($P < 0.001$), NO ($P = 0.006$), NC ($P = 0.003$), C ($P = 0.010$), P ($P = 0.007$), AL ($P < 0.001$), and ITC index ($P < 0.001$) among the three groups. The PAC/PACG group had the shallowest ACD, highest IOP, and greatest ITC index (all $P < 0.05$).

Lens parameters of three groups are presented in Table 2. Significant differences were detected for front Rs (normal vs PACS vs PAC/PACG: 8.91 ± 1.10 mm vs 8.07 ± 0.58 mm vs 7.81 ± 0.51 mm; $P < 0.001$), front Rf (normal vs PACS vs PAC/PACG: 9.80 ± 1.42 mm vs 8.73 ± 0.72 mm vs 8.44 ± 0.61 mm; $P < 0.001$), front R (normal vs PACS vs PAC/PACG: 9.35 ± 1.29 mm vs 8.40 ± 0.62 mm vs 8.12 ± 0.54 mm; $P < 0.001$), lens decentration (normal vs PACS vs PAC/PACG: 0.14 ± 0.07 mm vs 0.19 ± 0.09 mm vs 0.22 ± 0.12 mm; $P = 0.004$), lens tilt (normal vs PACS vs PAC/PACG: 4.9 ± 1.0° vs 5.3 ± 1.2° vs 5.8 ± 1.8°; $P = 0.033$), LT (normal vs PACS vs PAC/PACG: 4.57 ± 0.28 mm vs 4.87 ± 0.33 mm vs 4.96 ± 0.25 mm; $P < 0.001$), and LV (normal vs PACS vs PAC/PACG: 0.47 ± 0.30 mm vs 0.80 ± 0.22 mm vs 0.91 ± 0.21 mm; $P < 0.001$) among the three groups. The PACS and PAC/PACG groups had steeper front Rs, front Rf, front R, thicker LT, greater decentration and LV compared with the normal groups (all $P < 0.05$). The PAC/PACG groups had greater lens tilt when comparing the normal groups ($P = 0.034$). However, no statistically significant differences in back Rs ($P = 0.474$), back Rf ($P = 0.152$), back R ($P = 0.502$), or diameter ($P = 0.856$) of the lens were observed.

A Spearman analysis was conducted to determine the correlation of other factors associated with lens parameters (Table 3). Front Rs, front Rf, and front R were significantly associated with the stages of PACD, MSE, ACD, LV, AL, and the ITC index (all $P < 0.001$). LT was significantly associated with the stage of PACD, age, BCVA, ACD, LV, the grade of lens opacity (NO, NC, C, P), AL, and the ITC index (all $P < 0.05$). Decentration was significantly associated with the stage of PACD, age, BCVA, ACD, LV, NC, C, AL, and the ITC index (all $P < 0.05$). Tilt was significantly associated the stage of PACD, BCVA, MSE, ACD, the grade of lens opacity (NO, NC, C, P), AL, and the ITC index (all $P < 0.05$). No correlation was noted between lens parameters and sex or IOP.

Restricted cubic spline was used to estimate the dose–response relation of the ITC index and lens parameters. We found that the ITC index was negatively correlated with front Rs, front Rf, and front R; and positively correlated with LT, decentration, and tilt after adjustment for age, sex, and AL (Fig. 3), which indicated the ITC index was positively

Table 2. The Lens Parameters of Three Groups

Variables	Normal ($n = 38$)	PACS ($n = 57$)	PAC/PACG ($n = 30$)	*P* Value*
Front Rs, mm	8.91 ± 1.10	8.07 ± 0.58	7.81 ± 0.51	<0.001
Front Rs Axis, °	112.2 ± 38.9	106.9 ± 46.7	119.6 ± 40.8	0.471
Front Rf, mm	9.80 ± 1.42	8.73 ± 0.72	8.44 ± 0.61	<0.001
Front Rf Axis, °	60.1 ± 52.6	64.3 ± 48.2	59.6 ± 45.3	0.808
Front R, mm	9.35 ± 1.29	8.40 ± 0.62	8.12 ± 0.54	<0.001
Back Rs, mm	5.44 ± 0.38	5.38 ± 0.38	5.36 ± 0.41	0.474
Back Rs Axis, °	117.8 ± 57.5	99.0 ± 60.4	124.4 ± 49.2	0.095
Back Rf, mm	5.83 ± 0.42	5.71 ± 0.38	5.78 ± 0.42	0.152
Back Rf Axis, °	70.4 ± 36.7	75.3 ± 42.0	76.4 ± 42.5	0.910
Back R, mm	5.64 ± 0.38	5.54 ± 0.37	5.57 ± 0.36	0.502
Thickness, mm	4.57 ± 0.28	4.87 ± 0.33	4.96 ± 0.25	<0.001
Diameter, mm	9.97 ± 0.42	9.96 ± 0.36	10.0 ± 0.42	0.856
Decentration, mm	0.14 ± 0.07	0.19 ± 0.09	0.22 ± 0.12	0.004
Decentration axis, °	173.3 ± 63.2	173.6 ± 40.0	181.1 ± 51.3	0.814
Tilt, °	4.9 ± 1.0	5.3 ± 1.2	5.8 ± 1.8	0.033
Tilt axis, °	198.3 ± 16.1	194.5 ± 14.9	201.2 ± 23.7	0.382
LV, mm	0.47 ± 0.30	0.80 ± 0.22	0.91 ± 0.21	<0.001

Values are mean ± standard deviation.
* Differences between groups were tested with the Kruskal-Wallis test.

Table 3. The Association of Lens Parameters by Spearman Analysis

	Front Rs		Front Rf		Front R		Thickness		Decentration		Tilt	
Factors	r	*P* Value	r	*P* Value	r	*P* Value	r	*P* Value	r	*P* Value	r	*P* Value
Stage of PACD	−0.454	<0.001	−0.444	<0.001	−0.464	<0.001	0.447	<0.001	0.285	0.001	0.232	0.009
Age, years	0.025	0.780	0.012	0.893	0.024	0.790	0.388	<0.001	0.204	0.022	0.156	0.081
Sex (male:female)	−0.056	0.538	−0.023	0.893	−0.032	0.726	0.064	0.477	−0.114	0.207	0.012	0.893
BCVA, logMAR	−0.140	0.119	−0.157	0.081	−0.147	0.103	0.201	0.025	0.195	0.029	0.301	0.001
MSE, diopters	−0.301	0.001	−0.215	0.016	−0.259	0.004	0.101	0.264	0.120	0.182	0.192	0.032
IOP, mm Hg	−0.145	0.107	−0.136	0.130	−0.135	0.133	0.008	0.993	0.092	0.306	0.093	0.301
ACD, mm	0.661	<0.001	0.624	<0.001	0.664	<0.001	−0.593	<0.001	−0.393	<0.001	−0.180	0.045
CCT, µm	−0.046	0.614	0.002	0.98	−0.016	0.857	0.012	0.89	−0.076	0.397	−0.126	0.161
LV, mm	−0.681	<0.001	−0.635	<0.001	−0.671	<0.001	0.583	<0.001	0.318	<0.001	0.148	0.099
NO	−0.097	0.283	−0.13	0.149	−1.09	0.23	0.374	<0.001	0.160	0.075	0.207	0.021
NC	−0.111	0.219	−0.14	0.12	−0.121	0.18	0.37	<0.001	0.198	0.028	0.213	0.017
C	−0.145	0.107	−0.15	0.094	−0.144	0.108	0.403	<0.001	0.207	0.021	0.189	0.035
P	−0.151	0.093	−0.166	0.064	−0.157	0.081	0.387	<0.001	0.138	0.125	0.195	0.030
AL, mm	0.529	<0.001	0.512	<0.001	0.535	<0.001	−0.176	<0.001	−0.269	0.002	−0.274	0.002
ITC index, %	−0.397	<0.001	−0.455	<0.001	−0.445	<0.001	0.282	0.001	0.309	<0.001	0.219	0.014

correlated with anterior curvature, LT, decentration, and tilt of lens. Moreover, multivariate regression of lens parameters showed Front Rs, front Rf, front R, LT, and decentration were associated with the stage of PACD in the crude model (Table 4), and nearly all of these associations remained statistically significant after adjusting for age, sex, and AL, expect for the lens tilt. We also performed the tests for trend by entering the stage of the PACD as continuous parameters in the models and found that the stage of the PACD was negatively correlated with front Rs, front Rf, and front R, and positively correlated with LT and decentration even after adjustment for age, sex, and AL (all $P < 0.05$).

Discussion

Previous studies have demonstrated that crystalline lens contributed to the pathogenesis of PACD.[5–7,21] In the present study, we used AS-OCT to further investigate the detailed lens morphologic features in the whole range of PACD by comparing the biometric parameters with healthy control eyes and among different stages. To the best of our knowledge, this is the first time that high-quality imaging has been used to show the lens morphologic features in all stages of PACD by AS-OCT.

This cross-sectional study of 125 participants, which included 38 controls, 57 PACS, and 30 PAC/PACG, showed that the PACD eyes had steeper anterior curvature of lens, thicker LT, higher LV, and greater decentration comparing to normal eyes. As an indicator of the stages of PACD, the ITC index was also found to be negatively correlated with anterior radius curvature of lens and positively correlated with LT, decentration, and tilt after adjustment for age, sex, and AL. Our results suggested that the morphology and position of the crystalline lens were different in the early and late stages of PACD eyes.

Owing to a technical problem, AS-OCT and ultrasound biomicroscopy were not able to simultaneously and quantitatively display the anterior and posterior surface of the lens

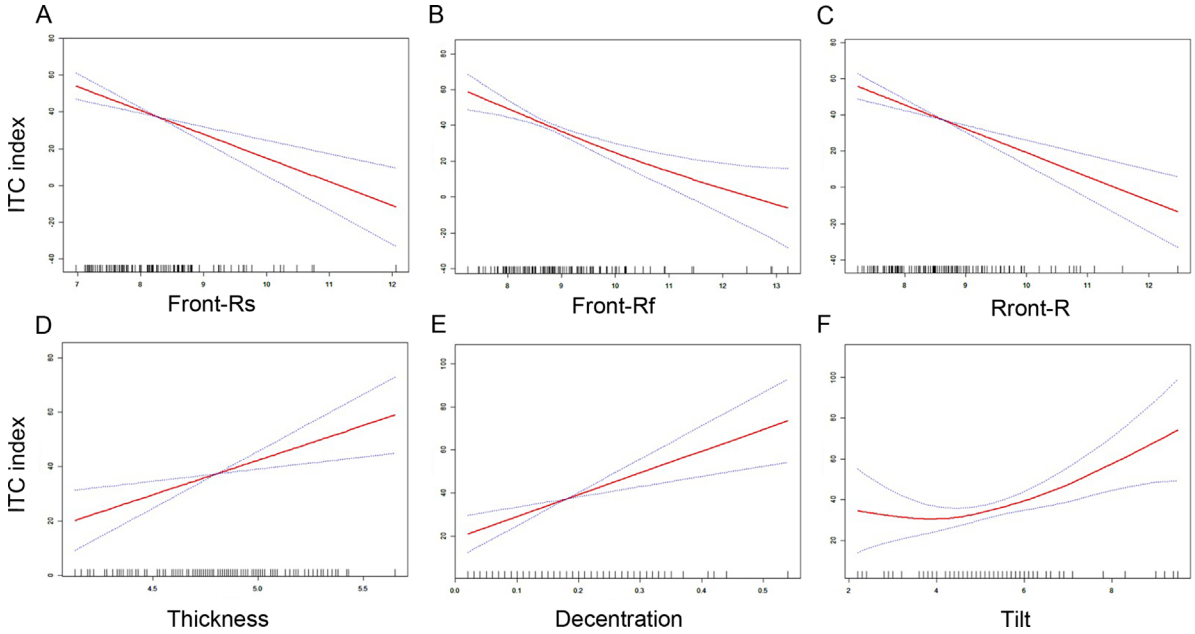

Figure 3. Restricted cubic spline analysis showed the relationship between ITC index (*y*-axis) and lens parameters (*x*-axis) after adjustment for age, sex, and AL, including front Rs (**A**), front Rf (**B**), front R (**C**), thickness (**D**), decentration (**E**), and tilt (**F**).

well. Previous studies of lens biometric parameters in PACD produced inconsistent results. There were studies that found that the PACD eyes had a greater iris–lens contact distance by ultrasound biomicroscopy,[22] a more anterior lens position (LP; defined as ACD + 1/2LT) by A-mode applanation ultrasonography,[23] and a greater LV by AS-OCT[24] compared with normal eyes. There was also one study that they did not find any difference of lens position when comparing angle closure eyes with those open angle eyes. Sihota et al.[15] found no differences in relative lens position (defined as LP/AL) when comparing PACG patients with family members. In our study, we demonstrated that the anterior radius curvature of the lens decreased, LV increased, LT increased, and the ACD decreased in the PACD eyes when compared with normal eyes. Because the curvature of the anterior lens surface, thickness of the lens, and relative lens position all partially rely on the tension of zonules, it is possible that the increase of lens curvature, LT, and LV are associated with zonular weakness, a finding that is also suggested by the phenomenon that patients with PACD are found to have high rate of zonular laxity in the cataract surgery.[25] Increased curvature of the anterior lens surface and LV likely increases the extent of iridolenticular contact, leading to a more significant pupillary block, and then angle crowding. In this study, we found that, even after adjustment for age, sex, and LV by the multivariate regression model, the stage of PACD was still negatively and significantly associated with the anterior radius curvature of lens (Supplementary Table S2). Therefore, in addition to the shallow ACD, shorter AL, and increased LT and LV, the increased curvature of anterior lens surface might be another anatomic characteristic of PACD eyes.

Another interesting finding in this study was that PACD eyes had a greater decentration of lens compared with normal eyes, which had a trend with the stage of PACD even after adjustment for age, sex, and AL. In this study, PACD eyes showed an average decentration of 0.22 ± 0.12 mm compared with 0.14 ± 0.07 mm in normal eyes. These results in normal eyes were consistent with the report from Kimura et al.,[20] which showed that normal eyes had an average decentration of 0.12 mm by using CASIA 2. However, so far, no report has been published about crystalline lens decentration in PACD eyes by AS-OCT. In addition, we observed that the extent of lens decentration is becoming more significant along with the stage of the disease. Because the well-centered position of the lens depends on the equal tension of zonules, the tilt and decentration of lens are probably related with the zonular weakness. The LPI could be effective in the early stage of such patients, because either anterior shift of lens or increasement of lens curvature would increase pupillary block, which can usually be relieved by LPI. However, these patients will eventually need surgery because the effect of LPI gradually wanes with the development of zonular weakness. Our results are also supported by the phenomenon that crystalline lens dislocation was frequently seen in PACG eyes, as reported by Zhang et al.[26] and Luo et al.[27] Although the tilt and decentration (PACG vs normal: 0.22 ± 0.12 mm vs 0.14 ± 0.07 mm) of the lens in PACG are small in our study, filtering surgery in PACG eyes may have increased risk of complications such as shallow anterior chamber and malignant glaucoma because of zonular weakness. Therefore, such patients should be more closely considered to treat with cataract surgery instead of filtering surgery. Meanwhile, more attention should be paid when cataract surgery is being performed due to the zonular weakness, and the capsular tension ring can be used to provide support to the lens capsule if necessary.

The present study was limited by its cross-sectional design, especially in that the number of participants was small in the PAC/PACG group, so the distribution of the lens morphologic parameters in PACD eyes may not represent the real development process during the progression of PACD. Moreover, the lens morphologic parameters in our study were calculated from certain formula provided by inbuilt

Table 4. Multivariate Regression for Lens Parameters

	Crude Model			Multivariate-Adjusted Model 1			Multivariate-Adjusted Model 2		
Variable	**β (95% CI)**	***P* Value**	***P* for Trend**	**β (95% CI)**	***P* Value**	***P* for Trend**	**β (95% CI)**	***P* Value**	***P* for Trend**
Front Rs									
Normal	Ref		<0.0001	Ref		<0.0001	Ref		<0.0001
PACS	−0.83 (−1.14 to −0.52)	<0.0001		−0.91 (−1.23 to −0.59)	<0.0001		−0.63 (−0.93 to −0.33)	<0.0001	
PAC/PACG	−1.09 (−1.46 to −0.73)	<0.0001		−1.19 (−1.57 to −0.82)	<0.0001		−0.86 (−1.21 to −0.50)	<0.0001	
Front Rf									
Normal	Ref		<0.0001	Ref		<0.0001	Ref		<0.0001
PACS	−1.07 (−1.46 to −0.67)	<0.0001		−1.17 (−1.58 to −0.77)	<0.0001		−0.87 (−1.27 to −0.48)	<0.0001	
PAC/PACG	−1.36 (−1.83 to −0.90)	<0.0001		−1.49 (−1.97 to −1.02)	<0.0001		−1.13 (−1.60 to −0.67)	<0.0001	
Front R									
Normal	Ref		<0.0001	Ref		<0.0001	Ref		<0.0001
PACS	−0.95 (−1.28 to −0.61)	<0.0001		−1.04 (−1.38 to −0.70)	<0.0001		−0.75 (−1.07 to −0.42)	<0.0001	
PAC/PACG	−1.23 (−1.62 to −0.84)	<0.0001		−1.34 (−1.74 to −0.94)	<0.0001		−0.99 (−1.38 to −0.61)	<0.0001	
Thickness									
Normal	Ref		<0.0001	Ref		<0.0001	Ref		<0.0001
PACS	0.30 (0.17 to 0.42)	<0.0001		0.27 (0.15 to 0.39)	<0.0001		0.25 (0.12 to 0.37)	0.0002	
PAC/PACG	0.39 (0.24 to 0.53)	<0.0001		0.35 (0.21 to 0.49)	<0.0001		0.33 (0.18 to 0.47)	<0.0001	
Decentration									
Normal	Ref		0.001	Ref		0.0055	Ref		0.0344
PACS	0.05 (0.01 to 0.09)	0.0144		0.04 (0.00 to 0.08)	0.0464		0.03 (−0.01 to 0.07)	0.1612	
PAC/PACG	0.07 (0.03 to 0.12)	0.0012		0.06 (0.02 to 0.11)	0.0061		0.05 (0.00 to 0.10)	0.035	
Tilt									
Normal	Ref		0.0031	Ref		0.0097	Ref		0.1309
PACS	0.42 (−0.12 to 0.96)	0.1272		0.33 (−0.22 to 0.87)	0.2409		0.03 (−0.52 to 0.58)	0.9104	
PAC/PACG	0.97 (0.34 to 1.60)	0.0031		0.86 (0.22 to 1.49)	0.0094		0.50 (−0.15 to 1.15)	0.1322	

The crude model adjusted for stage of PACD. Model 1 further adjusted for age and sex. Model 2 further adjusted for AL.

semiautomated software, which could potentially introduce bias. Direct measurement from complete imaging of the lens might provide more information.

In conclusion, our study demonstrated that PACD eyes had a steeper anterior curvature and greater decentration of lens when compared with normal eyes. The steep anterior curvature and decentered lens might be another anatomic characteristic in PACD eyes.

Acknowledgments

Supported by the State Program of National Natural Science Foundation of China (81570887, 81870692), the State Key Program of National Natural Science Foundation of China (81430007), the subject of major projects of National Natural Science Foundation of China (81790641), the Shanghai Committee of Science and Technology, China (17410712500), the top priority of clinical medicine center of Shanghai (2017ZZ01020). The sponsor or funding organization had no role in the design or conduct of this research.

Disclosure: **X. Wang,** None; **X. Chen,** None; **Y. Tang**, None; **J. Wang,** None; **Y. Chen,** None; **X. Sun,** None

References

1. Quigley HA. Number of people with glaucoma worldwide. *Br J Ophthalmol*. 1996;80:389–393.
2. Foster PJ, Johnson GJ. Glaucoma in China: how big is the problem? *Br J Ophthalmol*. 2001;85:1277–1282.
3. Cho HK, Kee C. Population-based glaucoma prevalence studies in Asians. *Surv Ophthalmol*. 2014;59:434–447.
4. Foster PJ, Buhrmann R, Quigley HA, Johnson GJ. The definition and classification of glaucoma in prevalence surveys. *Br J Ophthalmol*. 2002;86:238–242.
5. Lowe RF. Aetiology of the anatomical basis for primary angle-closure glaucoma. Biometrical comparisons between normal eyes and eyes with primary angle-closure glaucoma. *Br J Ophthalmol*. 1970;54:161–169.
6. Alsbirk PH. Primary angle-closure glaucoma. Oculometry, epidemiology, and genetics in a high risk population. *Acta Ophthalmol Suppl*. 1976;5–31.
7. Sihota R, Lakshmaiah NC, Agarwal HC, Pandey RM, Titiyal JS. Ocular parameters in the subgroups of angle closure glaucoma. *Clin Exp Ophthalmol*. 2000;28:253–258.
8. Anderson DR, Jin JC, Wright MM. The physiologic characteristics of relative pupillary block. *Am J Ophthalmol*. 1991;111:344–350.
9. Quigley HA, Friedman DS, Congdon NG. Possible mechanisms of primary angle-closure and malignant glaucoma. *J Glaucoma*. 2003;12:167–180.
10. Sun X, Dai Y, Chen Y, et al. Primary angle closure glaucoma: what we know and what we don't know. *Prog Retin Eye Res*. 2017;57:26–45.
11. Tomlinson A, Leighton DA. Ocular dimensions in the heredity of angle-closure glaucoma. *Br J Ophthalmol*. 1973;57:475–486.
12. Markowitz SN, Morin JD. The ratio of lens thickness to axial length for biometric standardization in angle-closure glaucoma. *Am J Ophthalmol*. 1985;99:400–402.
13. Salmon JF, Swanevelder SA, Donald MA. The dimensions of eyes with chronic angle-closure glaucoma. *J Glaucoma*. 1994;3:237–243.
14. Marchini G, Pagliarusco A, Toscano A, Tosi R, Brunelli C, Bonomi L. Ultrasound biomicroscopic and conventional ultrasonographic study of ocular dimensions in primary angle-closure glaucoma. *Ophthalmology*. 1998;105:2091–2098.
15. Sihota R, Ghate D, Mohan S, Gupta V, Pandey RM, Dada T. Study of biometric parameters in family members of primary angle closure glaucoma patients. *Eye (Lond)*. 2008;22:521–527.
16. Nongpiur ME, He M, Amerasinghe N, et al. Lens vault, thickness, and position in Chinese subjects with angle closure. *Ophthalmology*. 2011;118:474–479.
17. Ang LP, Aung T, Chew PT. Acute primary angle closure in an Asian population: long-term outcome of the fellow eye after prophylactic laser peripheral iridotomy. *Ophthalmology*. 2000;107:2092–2096.
18. Husain R, Do T, Lai J, et al. Efficacy of phacoemulsification alone vs phacoemulsification with goniosynechialysis in patients with primary angle-closure disease: a randomized clinical trial. *JAMA Ophthalmol*. 2019;137:1107–1113.
19. Chylack LT, Jr., Wolfe JK, Singer DM, et al. The Lens Opacities Classification System III. The Longitudinal Study of Cataract Study Group. *Arch Ophthalmol*. 1993;111:831–836.
20. Kimura S, Morizane Y, Shiode Y, et al. Assessment of tilt and decentration of crystalline lens and intraocular lens relative to the corneal topographic axis using anterior segment optical coherence tomography. *PLoS One*. 2017;12:e0184066.
21. Li M, Chen Y, Chen X, et al. Differences between fellow eyes of acute and chronic primary angle closure (glaucoma): an ultrasound biomicroscopy quantitative study. *PLoS One*. 2018;13:e0193006.
22. Mansoori T, Balakrishna N. Anterior segment morphology in primary angle closure glaucoma using ultrasound biomicroscopy. *J Curr Glaucoma Pract*. 2017;11:86–91.
23. Lim MC, Lim LS, Gazzard G, et al. Lens opacity, thickness, and position in subjects with acute primary angle closure. *J Glaucoma*. 2006;15:260–263.
24. Liu L, Liu X, Huang C, et al. Associated factors of acute primary angle closure glaucoma in a sub-group of Chinese people: comparison between attack eyes and normal controls. *Sci Rep*. 2017;7:14885.
25. Kubota T, Touguri I, Onizuka N, Matsuura T. Phacoemulsification and intraocular lens implantation combined with trabeculotomy for open-angle glaucoma and coexisting cataract. *Ophthalmologica*. 2003;217:204–207.
26. Zhang Y, Zong Y, Jiang Y, Jiang C, Lu Y, Zhu X. Clinical features and efficacy of lens surgery in patients with lens subluxation misdiagnosed as primary angle-closure glaucoma. *Curr Eye Res*. 2019;44:393–398.
27. Luo L, Li M, Zhong Y, Cheng B, Liu X. Evaluation of secondary glaucoma associated with subluxated lens misdiagnosed as acute primary angle-closure glaucoma. *J Glaucoma*. 2013;22:307–310.